

1 Infectious bronchitis coronavirus inhibits STAT1 signalling and requires accessory
2 proteins for resistance to type I interferon

3
4 Joeri Kint^{1,2}, Annemiek Dickhout¹, Jasmin Kutter¹, Helena J. Maier³, Paul Britton³, Joseph
5 Koumans², Gorben P. Pijlman⁴, Jelke J. Fros⁴, Geert F Wiegertjes¹, Maria Forlenza^{1, #}

6
7 ¹Cell Biology and Immunology Group, Wageningen Institute of Animal Sciences, Wageningen
8 University, Wageningen, The Netherlands.

9 ²MSD Animal Health, Bioprocess Technology & Support, Boxmeer, The Netherlands

10 ³Avian Viral Diseases, The Pirbright Institute, Compton Laboratory, United Kingdom.

11 ⁴Laboratory of Virology, Wageningen University, Wageningen, The Netherlands

12
13 [#] Correspondence should be addressed to M.F. (maria.forlenza@wur.nl)

14
15
16 **Abstract**

17 The innate immune response is the first line of defence against viruses and the type I interferon
18 (IFN) is a critical component of this response. Similar to other viruses, the *Gammacoronavirus*
19 infectious bronchitis virus (IBV) has evolved under evolutionary pressure to evade and counteract
20 the IFN response to enable its survival. Previously, we reported that IBV induces a delayed
21 activation of the IFN response. In the present work, we describe the resistance of IBV to IFN and
22 the potential role of accessory proteins herein. We show that IBV is fairly resistant to the antiviral
23 state induced by IFN and identify that the viral accessory proteins 3a is involved in resistance to
24 IFN, as its absence renders IBV less resistant to IFN treatment. In addition to this, we find that
25 independently of its accessory proteins, IBV inhibits IFN-mediated phosphorylation and
26 translocation of STAT1. In summary, we show that IBV uses multiple strategies to counteract the
27 IFN response.

28
29 **Importance**

30 In the present study we show that infectious bronchitis virus (IBV) is resistant to IFN treatment
31 and identify a role for the accessory proteins 3a in the resistance against the type I IFN response.
32 We also demonstrated that, in a time-dependent manner, IBV effectively interferes with IFN
33 signalling and that accessory proteins are dispensable for this activity. This study demonstrates
34 that the *Gammacoronavirus* IBV, similar to its mammalian counterparts, has evolved multiple
35 strategies to efficiently counteract the IFN response of its avian host, and identifies accessory
36 protein 3a as multifaceted antagonist of the avian IFN system.

37 Introduction

38 Infectious bronchitis virus (IBV) is a member of the genus *Gammacoronavirus*, a group of viruses
39 from the order of *Nidovirales* characterised by a large positive-stranded RNA genome (1). IBV is
40 the causative agent of infectious bronchitis, which is one of the most important viral diseases in
41 chickens, causing a highly contagious respiratory disease that can spread to the gastrointestinal or
42 the urogenital tract (2, 3). Despite widespread application of inactivated and live-attenuated
43 vaccines, IBV remains one of the most reported diseases in poultry farms worldwide.
44 Notwithstanding the widespread nature and economic importance of this virus, interactions
45 between IBV and the host immune response remain poorly understood.

46 During the immune response to viruses, the type I interferon response plays a pivotal role.
47 Recently, we have shown that IBV induces delayed activation of the interferon response (4) in a
48 manner similar to several members of the genus *Betacoronavirus*, including mouse hepatitis virus
49 (MHV), severe acute respiratory syndrome-associated coronavirus (SARS-CoV) and Middle East
50 respiratory syndrome coronavirus (MERS-CoV) (5-8). The observation that coronaviruses delay
51 activation of the IFN response and limit production of IFN, suggests that IFN has the ability to
52 hinder their propagation. In apparent contrast, most coronaviruses are relatively resistant to
53 treatment with IFN *in vitro* (9, 10), one exception being MERS-CoV, which was shown to be highly
54 sensitive to IFN β *in vitro* (11, 12). Although previous studies suggest that treatment with IFN could
55 hinder propagation of IBV, based on reduced plaque formation (13) and reduced syncytia formation
56 (14), quantitative data on the resistance of IBV to IFN is lacking.

57 To date, it is unknown which of the IBV proteins confer resistance to IFN, if any. Various studies
58 have demonstrated that accessory proteins of coronaviruses play an important role in the
59 resistance to the IFN-induced antiviral response (10, 12, 15-20). The accessory proteins of
60 coronaviruses are small (50 – 300 aa) proteins that are not essential for virus replication *in vitro*
61 (21). The number of accessory proteins varies between coronaviruses, and amino acid sequences
62 of accessory proteins from different genera show very limited similarity, suggesting that their
63 function is virus- or host specific. IBV has been shown to express at least four accessory proteins,
64 3a, 3b, 5a and 5b, which are translated from two polycistronic mRNAs. Recently, we showed that
65 both 3a and 3b limit transcription of *Ifn β* and that 3b limits production of IFN protein *in vitro* (4).
66 Additional roles of IBV accessory proteins have remained elusive.

67 In the present study we show that IBV is relatively resistant to treatment with either IFN α or IFN β ,
68 but that knockout of 3a makes IBV less resistant to treatment with type I IFN. In addition, we
69 show that IBV inhibits phosphorylation and translocation of the IFN-activated transcription factor

STAT1 and inhibits subsequent IFN-mediated activation of an ISG promoter, at least during late stages of the infection. However, using mutant viruses we demonstrate that the presence of accessory proteins 3a, 3b, 5a and 5b is not required for either inhibition of STAT1 translocation or activation of an ISG promoter. We discuss two strategies by which IBV counteracts the type I IFN response: one based on counteracting the IFN-mediated antiviral response using accessory protein 3a and another based on blocking of IFN-mediated activation of antiviral genes through inhibition of STAT1 translocation. This study demonstrates that the *Gammacoronavirus* IBV has evolved multiple strategies to counteract activation of, and clearance by the type I IFN response.

Materials and methods

Cells

Chicken embryonic kidneys (CEK) were aseptically removed from 17- to 19-day-old chicken embryos (Charles River, SPAFAS). A cell suspension was obtained by trypsinisation of kidneys for 30 min at 37 °C and subsequent filtration through a 100 µm mesh. The resulting CEK cells were seeded at 4×10^5 cells/cm² in a 1:1 mix of 199 and F10 medium (Invitrogen) supplemented with 0.5% fetal bovine serum (FBS), 0.1 % tryptose phosphate broth, 0.1% sodium bicarbonate, 0.1% HEPES and 1% penicillin-streptomycin (PenStrep; Gibco, Invitrogen). DF-1 chicken fibroblast cells, the African green monkey Vero cells and baby hamster kidney (BHK) cells were cultured in DMEM (Gibco, Invitrogen) supplemented with 10% fetal bovine serum (FBS) and 1% PenStrep. All cells were incubated in a humidified incubator at 37 °C and 5% CO₂.

Viruses

IBV Beaudette, strain Beau-R, as well as the generation of the ScAUG3a, ScAUG3b, ScAUG3ab, Δ3ab and ScAUG5ab viruses were described previously (22-24). In the ScAUG viruses, the start codons of the indicated accessory genes were mutated to stop codons. In the Δ3ab virus, ORF 3a and all except the final 17 nucleotides of ORF 3b have been deleted (22). The presence of second-site mutations and the absence of protein expression was verified for the applied batch. IBV was amplified on CEK cells and SinV was amplified on BHK cells. All viruses were titrated on the respective cell type on which the experiment was performed using the TCID₅₀ method as previously described (25).

103 **Immunohistochemistry**

104 Vero cells were cultured on 8 well Lab-Tek #1.0 borosilicate coverglasses (Sigma-Aldrich) whereas
105 CEK cells were cultured in 24-well culture plates. Briefly, cells were fixed with 3.7%
106 paraformaldehyde and permeabilized using 0.1% Triton X-100 in phosphate-buffered saline (PBS).
107 SinV infection was detected using a mouse monoclonal antibody against dsRNA (English & Scientific
108 Consulting) and IBV infection using antibodies against the IBV-nucleocapsid (N) protein (Prionics).
109 Tyr701-phosphorylated STAT1 (pSTAT1) was detected using the rabbit monoclonal antibody MA5-
110 15071 (Thermo Scientific) and total STAT1 was detected using the rabbit polyclonal antibody sc-
111 346 (Santa Cruz Biotechnology). Visualization was performed using Alexa-488 or -568 labelled
112 goat-anti-mouse or goat-anti-rabbit antibodies (Invitrogen). Antibodies were diluted 1:1000 in PBS
113 supplemented with 5% FBS, except the anti-pSTAT1 which was diluted 1:500. Nuclei were stained
114 with 4',6-diamidino-2-phenylindole (DAPI, 0.5 µg/ml; Sigma). Cells were imaged using a Zeiss
115 Primo Vert microscope and Axiovision software. Image overlays and cross-sections were made in
116 ImageJ. To evaluate the effects of IBV on STAT1 translocation to the nucleus, the presence of
117 (phospho)-STAT1 in the nucleus was quantified in wells that were first infected with the appropriate
118 virus strain and then stimulated with IFN. Within these wells, infected cells were identified using
119 the anti-IBV-N antibody and the percentage of nuclei showing translocation of (phospho)-STAT1 in
120 both infected and uninfected cells was calculated based on >500 cells from multiple images.

121

122 **Interferon sensitivity assay**

123 CEK, DF-1, or Vero cells at 100% confluency were pre-treated for 6 hours with different
124 concentrations of recombinant chicken IFN α or IFN β produced in HEK293 cells (26), or recombinant
125 human IFN α A/D (Sigma-Aldrich) or human IFN β (CalBioChem). Infections were carried out using
126 different viruses at the indicated MOI for two hours, after which cells were washed three times with
127 PBS and new medium containing the same concentration of interferon was added. Supernatants
128 were collected for titration at 18 hours post infection (hpi) (CEK) or 24 hpi (DF-1). IFN post-
129 treatment was performed in CEK cells that were first infected for 2h at an MOI 10, washed three
130 times with PBS, and subsequently, incubated with medium containing interferon. Supernatants
131 were collected for titration at 18 hpi.

132

133 **Quantification of viral RNA**

134 RNA was isolated from tissue culture supernatant on the MagNA Pure 96 Instrument using the
135 MagNA Pure 96 DNA and Viral Nucleic Acid Small Volume Kit (Roche Diagnostic) and the Viral NA

136 Universal SV 2.0 protocol. RT-qPCR was performed on 5 μ l RNA using the SYBR Green One-Step Kit
137 (Biorad) in a Bio-Rad CFX96 PCR apparatus. Primers against the nucleocapsid gene of IBV, based
138 on genbank sequence AY851295, were as previously published (4). Forward primer:
139 GAAGAAAACCGTCCCAGA, Reverse primer: TTACCAGCAACCCACAC.

140

141 **ISG54-luciferase reporter assays**

142 Vero or DF-1 cells were seeded at 80-90% confluence in 96 well plates and transfected using
143 FuGENE HD (Promega) at a 1:3.5 ratio of DNA:FuGENE HD according to manufacturers'
144 specifications. Per well, 100 ng of ISG54-luciferase reporter plasmid (kind gift from David E. Levy
145 (27)) was transfected, together with 2 ng pRL-SV40 Renilla plasmid (Promega) to correct for
146 differences in transfection efficiency and transcription. At least 24 hours later, cells were infected
147 and at various time points after infection, stimulated with 1000 U/ml IFN for an additional 6 hours.
148 Firefly and Renilla luciferase activities were quantified using the Dual-Glo Luciferase Assay
149 (Promega) and a Filtermax F5 luminometer (Molecular Devices). Luciferase activity was calculated
150 relative to the non-IFN-stimulated control showing the maximum activity in non-infected wells and
151 calculating the relative percentage in virus-infected wells.

152

153 **Western Blot**

154 Vero cells in 24 well plates at 90% confluency were infected with IBV Beau-R at MOI 1. At 18 hpi,
155 cells were stimulated with human IFN β (10,000 U/ml) for 30 min and subsequently lysed in lysis
156 buffer (20 mM Tris, 100 mM NaCl, 1mM EDTA, 0.5% Triton X-100 and 1 mM PMSF, pH 8.0).
157 Samples were boiled for 10 minutes in Laemmli loading buffer, clarified by centrifugation at 5000 x
158 g for 5 min and separated on a 10% SDS-PAGE gel. Proteins were transferred onto a Whatman
159 Protran nitrocellulose membrane (GE Healthcare) by semi-dry blotting (Trans-Blot SD Semi-Dry
160 Transfer Cell, Bio-Rad). Blotted membranes were blocked overnight in 5% non-fat dry milk (w/v) in
161 TBS/Tween (20 mM Tris, 500 mM NaCl, 0.05% Tween-20 (v/v), pH 8.0) at 4 °C. The blotted
162 membranes were incubated with primary antibodies (rabbit anti-STAT1 sc-346, Santa Cruz
163 Biotechnology 1:1000; rabbit anti-pSTAT1 MA5-15071, Thermo-Scientific 1:500; rabbit anti- β -
164 tubulin, Abcam, Ab6046 1:2000) in 5% non-fat dry milk in TBS/Tween for 1 h at 37 °C followed by
165 incubation with a goat-anti-rabbit-HRP antibody (Bio-Rad) at a 1:1000 dilution in the same buffer
166 for 1 h at 37 °C. Chemiluminescence of bound anti-rabbit-HRP antibody was detected with
167 WesternBright ECL (Advansta) and visualized using Lumni-film (Roche). Quantification of band
168 intensity was performed using imageJ software.

169 **Statistics**

170 Statistical analyses were performed in GraphPad Prism 6.0 or IBM SPSS 19. Equality of variance
171 was assessed using Bartlett's test. Significant differences were determined by a one-way ANOVA
172 followed by a Bonferroni or Tukey post-hoc test or by a two-way ANOVA when indicated.
173

174 **Results**

175 **IBV is relatively resistant to treatment with type I IFN**

176 To test resistance of IBV to type I IFN, we treated primary chicken embryo kidney (CEK) cells or
177 Vero cells with recombinant chicken IFN and subsequently infected them with IBV Beau-R, or with
178 the IFN-sensitive Sindbis virus as control. Immunofluorescence staining indicated that in both cell
179 types, propagation of IBV was less affected by treatment with IFN α and IFN β than propagation of
180 the IFN-sensitive Sindbis virus (Fig. 1A). To investigate the degree of IBV resistance to IFN, we
181 treated CEK cells with increasing concentrations of IFN α and IFN β , and determined the effect on
182 propagation by titration of Beau-R (Fig. 1B). The titre of Beau-R decreased in a dose-dependent
183 manner and in CEK cells, the effect of IFN β on the titre of Beau-R was more pronounced than that
184 of IFN α . Similar to other coronaviruses, relatively high concentrations of IFN (>1000 U/ml) were
185 required to hinder propagation of IBV Beau-R which suggested that IBV, like other coronaviruses,
186 is relatively resistant to IFN and raised the possibility that IBV actively counteracts the type I IFN
187 response.

188

189 **Accessory proteins 3a contributes to IFN resistance**

190 For coronaviruses other than IBV, the accessory proteins have been implicated in counteracting the
191 type I IFN response. To investigate whether the accessory proteins of IBV contribute to resistance
192 to IFN, we stimulated CEK cells with a high concentration of IFN (*IFN before virus*, inset), and
193 infected them with 3a/3b and 5a/5b null viruses (ScAUG3ab and ScAUG5ab). These viruses do not
194 express the indicated accessory proteins owing to a mutation in the AUG start codons. IFN
195 treatment reduced titres of ScAUG3ab more than that of either ScAUG5ab or the parental Beau-R
196 virus (Fig. 1C), suggesting that ScAUG3ab is more sensitive to treatment with IFN. Next, we
197 investigated whether absence of 3a and 3b would increase sensitivity of IBV to IFN-treatment after
198 the infection has been established (*IFN after virus*, inset). We synchronously infected CEK cells
199 using a high MOI of Beau-R, ScAUG3ab or ScAUG5ab virus. At 2hpi, cells were incubated with high
200 doses of IFN α and IFN β for an additional 16 hours, when infectious virus titres were determined by
201 titration of the supernatant (Fig.1D). The results show that, once infection has been established,
202 Beau-R is resistant to IFN treatment and that absence of accessory proteins 3a and 3b leads to a
203 marginal, but significant increase in sensitivity of IBV to IFN at least upon IFN β treatment.
204 To further investigate IFN-sensitivity of ScAUG3ab, we stimulated DF-1 cells with increasing
205 concentrations of IFN α or IFN β (Fig. 1E and 1F). Again, ScAUG3ab was more sensitive to treatment
206 with either IFN α or IFN β than ScAUG5ab or the parental Beau-R, indicating that accessory proteins

207 3a and/or 3b could play an important role in conferring resistance of IBV to treatment with type I
208 IFN in either chicken or mammalian cells. To further investigate whether accessory protein 3a, 3b
209 or both are responsible for the observed increase in IFN sensitivity, we stimulated DF-1 cells with
210 10.000 U/ml of IFN α or IFN β and infected them with individual mutants for either accessory protein
211 3a or 3b (ScAUG3a and ScAUG3b). As a control we included ScAUG3ab and delta 3a/3b (Δ 3ab)
212 viruses. The latter was obtained by deleting the open reading frames of both 3a and 3b (22) and
213 this virus was used to verify that IFN sensitivity of ScAUG3ab was not due to a second-site
214 mutation in the genome of this virus. Our results show that both ScAUG3a and ScAUG3b were
215 more sensitive to IFN treatment than Beau-R, but the effects on ScAUG3a virus were more
216 pronounced. To further investigate the difference in IFN-sensitivity between ScAUG3a and
217 ScAUG3b we quantified viral RNA in the supernatant of DF-1 cells pre-treated with increasing
218 concentration of IFN (Fig. 1H and 1I). We found that reduction of viral RNA was most prominent in
219 supernatants of cells infected with ScAUG3a and ScAUG3ab especially after IFN β treatment. Taken
220 together, we conclude that accessory protein 3a is the main contributor to resistance of IBV to type
221 I IFN.

222

223 **IBV prevents IFN signalling late during infection**

224 Next, we wanted to investigate how accessory proteins 3a and, to a lesser extent, 3b contribute to
225 IFN resistance. One possibility is that the proteins interfere with signalling of IFN, in a similar
226 manner as accessory protein ORF6 of SARS-CoV which was shown to block IFN signalling through
227 inhibition of nuclear translocation of STAT1 (28). To investigate whether also IBV is able to inhibit
228 nuclear translocation of STAT1, we used Vero cells, as commercially available STAT1 antibodies did
229 not detect chicken STAT1. Vero cells were infected with IBV and translocation of STAT1 was
230 induced at 6 and 18 hpi by stimulation for 30 minutes with IFN β . Localisation of STAT1 in the
231 nucleus of IBV-infected cells was visualised by immunostaining against STAT1 (Fig. 2A). In mock-
232 treated cells (no stimulation with IFN β), nuclear translocation of STAT1 was not visible, neither in
233 infected nor in non-infected cells (black arrowheads), indicating that IBV infection alone does not
234 induce translocation of STAT1. At 6 hpi IBV did not prevent IFN β -induced translocation of STAT1
235 (white arrowheads). At 18 hpi however, IFN β -induced translocation of STAT1 was strongly reduced
236 in IBV-infected cells (Fig 2A, bottom row of images). This indicated that IBV-mediated inhibition of
237 STAT1 translocation is a time-dependent event.

238 To substantiate the observed time-dependency of IBV-mediated inhibition of STAT1 translocation,
239 we quantified translocation of STAT1 in pictures taken of IBV-infected monolayers, containing both

240 infected and non-infected cells, within IFN β -treated wells at various time points after IBV infection.
241 In non-infected cells (non-inf. cells), treatment with IFN β led to translocation of STAT1 in more
242 than 90% of the cells (Fig. 2B, black bars), regardless of time point (6-24 hpi) or presence of
243 neighbouring cells infected with IBV (not shown). Translocation of STAT1 in mock-treated cells was
244 comparable between IBV-infected and non-infected cells (<5%, data not shown), indicating that
245 IBV alone did not induce translocation of STAT1. In contrast, in IBV-infected cells (IBV inf. cells),
246 treatment with IFN β did not always lead to translocation of STAT1. The inhibition seen in IBV-
247 infected cells was time-dependent: at time points between 6 and 12 hpi translocation of STAT1 was
248 not different from non-infected cells, whereas at later time points, between 12-18 hpi onwards,
249 STAT1 translocation was strongly inhibited (Fig. 2B, black bars).

250 To verify whether the observed time-dependent IBV-mediated inhibition of STAT1 translocation
251 would correlate with inhibition of transcription of ISGs, we used an IFN reporter assay based on the
252 human *ISG54* promotor, that contains multiple copies of the STAT1-binding interferon-stimulated
253 response element (ISRE) driving expression of the luciferase gene (27). *ISG54*-luciferase-
254 transfected DF-1 cells were infected for 12h or 24h with IBV and in the last 6h of infection treated
255 with IFN β (Fig 2C, inset). Indeed, at early time points after infection (12 hpi) we observed only a
256 marginal inhibition of luciferase production, whereas at later time points (24 hpi) IBV strongly
257 inhibited the IFN-mediated production of luciferase to the same extent as Sindbis virus, a well-
258 known inhibitor of STAT signalling (Fig. 2C). We interpret inhibition of luciferase activity as the
259 result of a reduction in IFN-mediated *ISG54* promoter activity and thus conclude that IBV inhibited
260 the transcription of ISGs by inhibiting translocation of STAT1, but only during later stages of
261 infection.

262

263 **IBV inhibits phosphorylation of STAT1**

264 A crucial step in IFN-induced translocation of STAT1 is its phosphorylation. Only phosphorylated
265 STAT1 (pSTAT1) can associate with STAT2 and IRF9 to form the transcription factor ISGF3, which
266 binds to ISRE promoter elements. To investigate whether IBV is able to block phosphorylation of
267 STAT1, we first performed a western blot analysis (Fig. 3A). Levels of total STAT1 were comparable
268 between IBV-infected and non-infected cells, whereas IFN β -mediated phosphorylation of STAT1
269 was reduced in infected compared to non-infected cells, confirming that IBV prevents
270 phosphorylation of STAT1 without affecting total STAT1 levels. In the western blot, we observed a
271 residual signal for pSTAT1 in IFN β -stimulated-IBV-infected cells, which was most likely due to the
272 presence of non-infected cells in the sample.

273 To better quantify the reduction in STAT1 phosphorylation observed in the western blot analysis,
274 we visualised IFN β -induced phosphorylation of STAT1 in IBV-infected cells (18 hpi), using a
275 pSTAT1-specific antibody. pSTAT1 could not be detected in mock-treated cells, even when infected
276 with IBV (Fig. 3B, upper panel; left). Cells treated with IFN β however (Fig. 3B, lower panel),
277 showed nuclear translocation of pSTAT1, but mostly in non-infected cells. In IBV-infected cells, in
278 contrast, translocation of pSTAT1 was severely reduced. In addition to reduced levels of nuclear
279 pSTAT1 (*i.e.* reduced translocation), we also observed reduced levels of cytoplasmic pSTAT1 in
280 IFN β -stimulated cells infected with IBV (Fig. 3C, delineated area). A cross-section of IBV-infected
281 areas versus non-infected areas confirmed the general lack of pSTAT1 signal in IBV-infected cells
282 (Fig 3C). Taken together, our data suggest that IBV prevents IFN-induced phosphorylation of
283 STAT1.

284

285 **IBV accessory proteins are not required for inhibition of phosphorylation and**
286 **translocation of STAT1.**

287 The *Betacoronavirus* SARS-CoV mediates inhibition of STAT1 translocation by its accessory protein
288 ORF6 (28, 29). To test whether the IBV accessory proteins are also involved in inhibition of
289 phosphorylation and translocation of STAT1, we used ScaUG3ab and ScaUG5ab viruses. First, we
290 investigated whether the accessory proteins of IBV are involved in inhibition of STAT1
291 phosphorylation. Western blot analysis indicated that wild-type Beau-R had a more pronounced
292 inhibitory effect on STAT1 phosphorylation than ScaUG5ab, whereas the inhibitory effect on
293 pSTAT1 of ScaUG3ab was intermediate (Fig. 4A). To confirm the increased phosphorylation of
294 STAT1 in ScaUG3ab and ScaUG5ab-infected cells, we performed immunostaining for pSTAT1. We
295 found that, contrary to the western blot analysis, both phosphorylation (Fig. 4B), as well as
296 translocation (Fig. 4C) of pSTAT1 appeared to be inhibited to the same extent by ScaUG3ab,
297 ScaUG5ab and Beau-R. To better compare inhibition of pSTAT1 translocation between ScaUG3ab,
298 ScaUG5ab and Beau-R, we performed image analysis of infected and non-infected cells within
299 infected monolayers after stimulation with IFN. Our results show that nuclear translocation of
300 pSTAT1 was inhibited to the same extent by all three viruses (Fig. 4D, black bars, IBV-inf. cells).
301 Nuclear translocation of pSTAT1 in non-infected cells within infected monolayers (non inf. cells)
302 was comparable between the three viruses. To explain the apparent discrepancy between the
303 levels of STAT1 phosphorylation observed in the western blot (Fig 4A) and in the STAT1
304 immunostaining (Fig 4B), we investigated the efficiency of replication of Beau-R, ScaUG3ab and
305 ScaUG5ab in Vero cells. To do so, we quantified the percentage of infected cells in microscopic

306 images (Fig 4E) in parallel to quantification of virus titre in supernatants of infected cells (Fig 4F).
307 These experiments indicated that replication of ScAUG5ab was less efficient than that of Beau-R
308 and ScAUG3ab, which is in agreement with a previous report showing that replication of ScAUG5ab
309 is reduced in Vero, but not in CEK cells (30). Reduced replication of ScAUG5ab in Vero cells
310 provides an explanation for its reduced inhibitory effect on IFN-mediated phosphorylation of STAT1
311 in the western blot analysis. In short, we conclude that both phosphorylation and nuclear
312 translocation of pSTAT1 is inhibited to the same extent by ScAUG3ab, ScAUG5ab and the parental
313 Beau-R virus. Next, we investigated to which extent ScAUG3ab and ScAUG5ab would inhibit IFN-
314 mediated activation of the ISG54 promoter and found no differences between ScAUG3ab and
315 ScAUG5ab and Beau-R, in both Vero and DF-1 cells (Fig. 4G). Taken together, our data indicate
316 that the inhibition of phosphorylation and translocation of STAT1 as well as activation of the ISG54
317 promoter, observed after infection with IBV, is independent of the accessory proteins 3a, 3b, 5a
318 and 5b.

319 **Discussion**

320 In this study we investigated the *in vitro* sensitivity of the *Gammacoronavirus* IBV to treatment
321 with IFN, and the potential role of IBV accessory proteins in conferring resistance to the host's type
322 I IFN response. We found IBV to be relatively resistant to either pre- or post-treatment with IFN
323 and showed that simultaneous knockout of the accessory proteins 3a and 3b decreased resistance
324 of IBV to IFN treatment. In addition, we present evidence that accessory protein 3a is primarily
325 responsible for the observed IFN resistance by IBV. Finally, we found that IBV interferes with IFN
326 signalling by inhibition of phosphorylation and nuclear translocation of STAT1 in a time-dependent
327 manner and that both 3a and 3b are dispensable for this activity. In summary, this study
328 demonstrates that the *Gammacoronavirus* IBV has evolved multiple strategies to antagonise the
329 innate immune response.

330 The coronaviruses MHV, SARS-CoV, MERS-CoV and IBV have all been shown to induce modest and
331 delayed transcription of *Ifn β* (8, 31). *Alpha-* and *Betacoronaviruses* (not *Gamma-* and
332 *Deltacoronaviruses*) encode the nsp1 protein that decreases transcription of *Ifn β* and inhibits
333 synthesis of host proteins thereby further reducing production of IFN (4, 32-35). The observation
334 that coronaviruses employ multiple strategies to limit production of IFN seems to suggest that IFN
335 could be detrimental to the propagation of coronaviruses. However, treatment of both MHV and
336 Feline coronavirus (FCoV) with IFN (1000 U) reduces their propagation by approximately 1 log only,
337 indicating that these viruses are relatively resistant to IFN (9, 36). In comparison, SARS-CoV is at
338 least 10 times more sensitive (37-39), and MERS-CoV even 1000 times more sensitive to IFN
339 treatment than MHV (11, 29). We found that propagation of IBV was reduced by 0.5 - 2.5 log upon
340 pre-treatment with IFN (1000 U) and less than 0.5 log upon IFN post-treatment suggesting that
341 IBV is relatively resistant to IFN especially when the infection has already been established. Our
342 results indicate that both the ScAUG3a and ScAUG3ab viruses are less resistant to IFN treatment
343 than the parental virus, whereas IFN-resistance of ScAUG3b was comparable to the parental virus.
344 These results indicate that, of the four accessory proteins of IBV, 3a is the protein that primarily
345 contributes to the resistance of IBV to IFN. Interestingly, it was previously shown that during
346 infection of primary chicken trachea organ culture (TOC), the titre of both ScAUG3a and ScAUG3ab
347 viruses declined more rapidly than that of the parental virus or ScAUG3b (22). In view of our
348 findings, the decrease in titre of ScAUG3a and ScAUG3ab in TOC could be the result of increased
349 sensitivity of both viruses to IFN produced by cells of the TOC.

350 Compared to MHV and FCoV, SARS-CoV is relatively sensitive to IFN treatment. However, MERS-
351 CoV is 50 to 100 times more sensitive than SARS-CoV (11, 29). The difference in sensitivity

352 between the latter two viruses has been ascribed to the ability of SARS-CoV to inhibit nuclear
353 translocation of pSTAT1 (29). Considering the relative resistance of IBV to treatment with IFN we
354 investigated whether IBV, similar to SARS-CoV, would inhibit nuclear translocation of pSTAT1. We
355 observed that at time points earlier than 18 hpi, IBV did not inhibit nuclear translocation of pSTAT1
356 or activation of a STAT1-responsive promoter (ISG54). In contrast, from 18 hpi onwards, IBV
357 inhibited both IFN-mediated pSTAT1 translocation and activation of the ISG54-promoter. Of
358 interest, SARS-CoV has been shown to inhibit STAT1 translocation as early as 8 hpi, whereas
359 MERS-CoV did not inhibit STAT1 translocation (29). In another study, MHV did not inhibit IFN-
360 mediated translocation of STAT1-GFP at 9 hpi, but inhibited IFN-mediated ISG expression at 11 hpi
361 and rescued Sendai virus (SeV) from the antiviral effects of IFN β when MHV was present prior to
362 SeV infection and for a total period of 16 h (5). Our data indicate a time-dependent inhibition of
363 IFN signalling by IBV, a phenomenon that has not been reported for other coronaviruses, although
364 it cannot be excluded that for the *Betacoronaviruses* MHV and possibly MERS-CoV, inhibition of
365 pSTAT1 translocation could be a relatively late event similar to what we observed for the
366 *Gammacoronavirus* IBV.

367 For SARS-CoV, it has been shown that accessory protein ORF6 is responsible for blocking nuclear
368 translocation of STAT1 by tethering nuclear import factors at the ER/Golgi membrane, inhibiting
369 expression of STAT1-activated genes (19, 28, 40). In the present study we showed that IBV
370 inhibits phosphorylation of STAT1 and that, in contrast to SARS-CoV, the presence of accessory
371 proteins of IBV was not required for inhibition of STAT1-mediated signalling. Our data suggest that
372 IBV and SARS-CoV may exploit different strategies to inhibit translocation of STAT1.

373 Taking together the ability of IBV to significantly delay transcription of *Ifn β* up until 12-18 hpi and
374 delay subsequent translation of IFN until 36 hpi (4) and the inhibition of pSTAT1 translocation at
375 times points >18 hpi, we suggest there could be a correlation between the timing of *Ifn β*
376 transcription by the host cell and inhibition of IFN signalling induced by IBV. Although there is no
377 proof of causality, we hypothesize that changes in the host cell trigger the relocation of, or
378 conformational changes in IBV proteins, which in turn activate their anti-IFN activity. Further
379 research is needed to verify this hypothesis.

380 In general, coronavirus accessory proteins have been shown to antagonise the IFN response at
381 various steps. For example, proteins 4a and 4b of MERS and 3b of SARS inhibit activation of *Ifn β*
382 (12, 16, 19), whereas protein 7 of TGEV and 3b of IBV inhibit transcription and translation of *Ifn β*
383 (4, 17, 41). Notwithstanding these and other steps to counteract and/or avoid activation of the IFN
384 response (reviewed in (42)), accessory proteins not only inhibit activation of the IFN response, but

385 they also antagonise the antiviral effect of IFN. ORF6 of SARS-CoV inhibits IFN-signalling by
386 blocking translocation of STAT1 (28), ns2 of MHV inhibits the IFN-activated OAS-RNase L antiviral
387 pathway (20) and 5a of MHV and 7a of FCoV also confer resistance to IFN treatment but via
388 presently unknown mechanisms (10, 18). Using IBV accessory protein null viruses, we show that
389 knockout of protein 3a renders IBV more sensitive to IFN treatment. In a previous study we found
390 that 3a decreases transcription of *Ifn β* and modulates production of IFN protein (4). The
391 mechanism by which accessory proteins 3a confers resistance to IFN treatment remains unclear
392 although, in the present study, we could show that 3a does not interfere with STAT1-mediated
393 signalling.

394 To explain the role of 3a in counteracting the type I IFN response, we hypothesise that 3a might
395 interact with host-proteins involved in both the induction of *Ifn β* as well as the IFN-induced
396 antiviral response. Host proteins that meet these criteria are, for example, the dsRNA-activated
397 antiviral proteins PKR and OAS. For MHV it was demonstrated that accessory protein ns2,
398 antagonises the 2'-5'-oligoadenylate synthetase (OAS) ribonuclease (RNase) L pathway (20); a
399 potent antiviral response activated by double-stranded RNA. Accessory protein 3a of IBV however,
400 does not contain the canonical HxT/S catalytic 2H-phosphoesterase motifs that are essential for the
401 IFN-antagonistic activity of ns2 (43). Interestingly, accessory protein 3a has been shown to
402 partially co-localise with dsRNA in IBV-infected chicken cells (44), which could indicate that 3a may
403 prevent the dsRNA-mediated activation of the OAS/RNase L pathway.

404
405 Coronaviruses induce extensive remodelling of intracellular membranes (45-47), a process that is
406 essential for coronavirus replication (48-50). It has been suggested that these membrane
407 structures shield dsRNA from the host cell (45, 51, 52), to avoid activation of the IFN response and
408 simultaneously shield nascent viral RNA from the activity of antiviral proteins (45, 52). The
409 shielding of dsRNA by membrane structures could explain both the delayed transcription of *Ifn β*
410 during MHV and IBV infections (8, 31) and the inability of these two coronaviruses to inhibit *Ifn β*
411 transcription induced by poly I:C or other RNA viruses (3, 32, 33). An alternative explanation for
412 their involvement in limiting IFN production and in resistance to IFN would be that 3a of IBV could
413 stabilize IBV-induced membrane structures. Absence of 3a would then lead to destabilisation of the
414 membrane structures allowing replicating IBV to be detected by antiviral-proteins and pattern
415 recognition receptors. Additional research is required to identify how exactly the IBV accessory
416 protein 3a counteracts the type I IFN response.

417 Taken together, the present study indicates that infectious bronchitis virus is relatively resistant to
418 treatment with IFN, at least *in vitro*, and suggests that IBV resists the antiviral activity of IFN via at
419 least two mechanisms: first, IBV inhibits IFN-mediated activation of antiviral genes through
420 inhibition of STAT1 phosphorylation and subsequent nuclear translocation in a time-dependent
421 manner. This inhibition occurs at relatively late time points after infection, correlating with
422 upregulation of *Ifn β* transcription (3). Second, IBV counteracts the IFN response primarily through
423 the action of the 3a protein. This study demonstrates that the *Gammacoronavirus* IBV, similar to
424 its mammalian counterparts, has evolved multiple strategies to efficiently counteract the IFN
425 response of its avian host, and identifies accessory protein 3a as an antagonist of the avian IFN
426 system.

427

428 **Acknowledgements:** This work was financially supported by MSD Animal Health, Bioprocess
429 Technology & Support, Boxmeer, The Netherlands. Helena Maier and Paul Britton were supported
430 by The Pirbright Institute and the Biotechnology and Biological Sciences Research Council (BBSRC).
431 The authors wish to thank Dr. EJ Bakker from the Mathematical and Statistical Methods Group of
432 Wageningen University and Dr. E van den Born from MSD Animal health for assistance with
433 statistical analysis and quantification of IBV RNA respectively.

434 References

- 435 1. **Gorbalenya AE, Enjuanes L, Ziebuhr J, Snijder EJ.** 2006. Nidovirales: evolving the largest RNA
436 virus genome. *Virus Res* **117**:17-37.
- 437 2. **Cavanagh D.** 2007. Coronavirus avian infectious bronchitis virus. *Vet Res* **38**:281-297.
- 438 3. **Britton P, and Cavanagh, D.** 2007. Avian coronavirus diseases and infectious bronchitis vaccine
439 development, , p 161-181. . *In* Thiel V (ed), *Coronaviruses: Molecular and Cellular Biology* Caister
440 Academic Press, Norfolk, UK.
- 441 4. **Kint J, Fernandez-Gutierrez M, Maier HJ, Britton P, Langereis MA, Koumans J, Wiegertjes GF,
442 Forlenza M.** 2015. Activation of the chicken type I interferon response by infectious bronchitis
443 coronavirus. *J Virol* **89**:1156-1167.
- 444 5. **Rose KM, Elliott R, Martinez-Sobrido L, Garcia-Sastre A, Weiss SR.** 2010. Murine coronavirus
445 delays expression of a subset of interferon-stimulated genes. *J Virol* **84**:5656-5669.
- 446 6. **Zhou H, Zhao J, Perlman S.** 2010. Autocrine interferon priming in macrophages but not dendritic
447 cells results in enhanced cytokine and chemokine production after coronavirus infection. *MBio* **1**.
- 448 7. **Devaraj SG, Wang N, Chen Z, Tseng M, Barretto N, Lin R, Peters CJ, Tseng CT, Baker SC, Li K.**
449 2007. Regulation of IRF-3-dependent innate immunity by the papain-like protease domain of the
450 severe acute respiratory syndrome coronavirus. *J Biol Chem* **282**:32208-32221.
- 451 8. **Menachery VD, Eisfeld AJ, Schafer A, Josset L, Sims AC, Proll S, Fan S, Li C, Neumann G,
452 Tilton SC, Chang J, Gralinski LE, Long C, Green R, Williams CM, Weiss J, Matzke MM, Webb-
453 Robertson BJ, Schepmoes AA, Shukla AK, Metz TO, Smith RD, Waters KM, Katze MG,
454 Kawaoka Y, Baric RS.** 2014. Pathogenic influenza viruses and coronaviruses utilize similar and
455 contrasting approaches to control interferon-stimulated gene responses. *MBio* **5**:e01174-01114.
- 456 9. **Roth-Cross JK, Martinez-Sobrido L, Scott EP, Garcia-Sastre A, Weiss SR.** 2007. Inhibition of the
457 alpha/beta interferon response by mouse hepatitis virus at multiple levels. *J Virol* **81**:7189-7199.
- 458 10. **Dedeurwaerder A, Olyslaegers DA, Desmaretts LM, Roukaerts ID, Theuns S, Nauwynck HJ.**
459 2013. The ORF7-encoded accessory protein 7a of feline infectious peritonitis virus as a counteragent
460 against interferon-alpha induced antiviral response. *J Gen Virol* doi:10.1099/vir.0.058743-0.
- 461 11. **Hart BJ, Dyal J, Postnikova E, Zhou H, Kindrachuk J, Johnson RF, Olinger GG, Frieman MB,
462 Holbrook MR, Jahrling PB, Hensley L.** 2013. Interferon-beta and mycophenolic acid are potent
463 inhibitors of Middle East respiratory syndrome coronavirus in cell-based assays. *Journal of General*
464 *Virology* doi:10.1099/vir.0.061911-0.
- 465 12. **Matthews KL, Coleman CM, van der Meer Y, Snijder EJ, Frieman MB.** 2014. The ORF4b-encoded
466 accessory proteins of MERS-Coronavirus and two related bat coronaviruses localize to the nucleus and
467 inhibit innate immune signaling. *J Gen Virol* doi:10.1099/vir.0.062059-0.
- 468 13. **Pei J, Sekellick MJ, Marcus PI, Choi IS, Collisson EW.** 2001. Chicken interferon type I inhibits
469 infectious bronchitis virus replication and associated respiratory illness. *J Interferon Cytokine Res*
470 **21**:1071-1077.
- 471 14. **Otsuki K, Maeda J, Yamamoto H, Tsubokura M.** 1979. Studies on avian infectious bronchitis virus
472 (IBV). III. Interferon induction by and sensitivity to interferon of IBV. *Archives of virology* **60**:249-255.
- 473 15. **Yang Y, Zhang L, Geng H, Deng Y, Huang B, Guo Y, Zhao Z, Tan W.** 2013. The structural and
474 accessory proteins M, ORF 4a, ORF 4b, and ORF 5 of Middle East respiratory syndrome coronavirus
475 (MERS-CoV) are potent interferon antagonists. *Protein Cell* **4**:951-961.
- 476 16. **Niemeyer D, Zillinger T, Muth D, Zieleski F, Horvath G, Suliman T, Barchet W, Weber F,
477 Drosten C, Muller MA.** 2013. Middle East respiratory syndrome coronavirus accessory protein 4a is a
478 type I interferon antagonist. *J Virol* **87**:12489-12495.
- 479 17. **Cruz J, Sola I, Becares M, Alberca B, Plana J, Enjuanes L, Zuniga S.** 2011. Coronavirus gene 7
480 counteracts host defenses and modulates virus virulence. *PLoS pathogens* **7**:e1002090.
- 481 18. **Koetzner CA, Kuo L, Goebel SJ, Dean AB, Parker MM, Masters PS.** 2010. Accessory protein 5a is
482 a major antagonist of the antiviral action of interferon against murine coronavirus. *J Virol* **84**:8262-
483 8274.
- 484 19. **Kopecky-Bromberg SA, Martinez-Sobrido L, Frieman M, Baric RA, Palese P.** 2007. Severe acute
485 respiratory syndrome coronavirus open reading frame (ORF) 3b, ORF 6, and nucleocapsid proteins
486 function as interferon antagonists. *Journal of Virology* **81**:548-557.
- 487 20. **Zhao L, Jha BK, Wu A, Elliott R, Ziebuhr J, Gorbalenya AE, Silverman RH, Weiss SR.** 2012.
488 Antagonism of the interferon-induced OAS-RNase L pathway by murine coronavirus ns2 protein is
489 required for virus replication and liver pathology. *Cell Host and Microbe* **11**:607-616.
- 490 21. **Narayanan K, Huang C, Makino S.** 2008. Coronavirus Accessory Proteins, Nidoviruses
491 doi:doi:10.1128/9781555815790.ch15. American Society of Microbiology.
- 492 22. **Hodgson T, Britton P, Cavanagh D.** 2006. Neither the RNA nor the proteins of open reading frames
493 3a and 3b of the coronavirus infectious bronchitis virus are essential for replication. *Journal of virology*
494 **80**:296-305.
- 495 23. **Casais R, Davies M, Cavanagh D, Britton P.** 2005. Gene 5 of the avian coronavirus infectious
496 bronchitis virus is not essential for replication. *Journal of virology* **79**:8065-8078.
- 497 24. **Casais R, Thiel V, Siddell SG, Cavanagh D, Britton P.** 2001. Reverse genetics system for the avian
498 coronavirus infectious bronchitis virus. *J Virol* **75**:12359-12369.
- 499 25. **Kint J, Maier HJ, Jagt E.** 2015. Quantification of infectious bronchitis coronavirus by titration in vitro
500 and in ovo. *Methods Mol Biol* **1282**:89-98.
- 501 26. **Schultz U, Rinderle C, Sekellick MJ, Marcus PI, Staeheli P.** 1995. Recombinant chicken interferon
502 from *Escherichia coli* and transfected COS cells is biologically active. *European journal of biochemistry*
503 **229**:73-76.
- 504 27. **Paulson M, Press C, Smith E, Tanese N, Levy DE.** 2002. IFN-Stimulated transcription through a
505 TBP-free acetyltransferase complex escapes viral shutoff. *Nat Cell Biol* **4**:140-147.

- 506 28. **Frieman M, Yount B, Heise M, Kopecky-Bromberg SA, Palese P, Baric RS.** 2007. Severe acute
507 respiratory syndrome coronavirus ORF6 antagonizes STAT1 function by sequestering nuclear import
508 factors on the rough endoplasmic reticulum/Golgi membrane. *J Virol* **81**:9812-9824.
- 509 29. **de Wilde AH, Raj VS, Oudshoorn D, Bestebroer TM, van Nieuwkoop S, Limpens RW,**
510 **Posthuma CC, van der Meer Y, Barcena M, Haagmans BL, Snijder EJ, van den Hoogen BG.**
511 2013. MERS-coronavirus replication induces severe in vitro cytopathology and is strongly inhibited by
512 cyclosporin A or interferon-alpha treatment. *J Gen Virol* **94**:1749-1760.
- 513 30. **Dent S.** 2014. Proteomic analysis of IBV Infection to study the effect of the accessory proteins 5a and
514 5b. PhD. University of Reading.
- 515 31. **Kindler E, Jonsdottir HR, Muth D, Hamming OJ, Hartmann R, Rodriguez R, Geffers R,**
516 **Fouchier RA, Drosten C, Muller MA, Dijkman R, Thiel V.** 2013. Efficient Replication of the Novel
517 Human Betacoronavirus EMC on Primary Human Epithelium Highlights Its Zoonotic Potential. *MBio* **4**.
- 518 32. **Kamitani W, Huang C, Narayanan K, Lokugamage KG, Makino S.** 2009. A two-pronged strategy
519 to suppress host protein synthesis by SARS coronavirus Nsp1 protein. *Nat Struct Mol Biol* **16**:1134-
520 1140.
- 521 33. **Huang C, Lokugamage KG, Rozovics JM, Narayanan K, Semler BL, Makino S.** 2011.
522 Alphacoronavirus transmissible gastroenteritis virus nsp1 protein suppresses protein translation in
523 mammalian cells and in cell-free HeLa cell extracts but not in rabbit reticulocyte lysate. *J Virol* **85**:638-
524 643.
- 525 34. **Zust R, Cervantes-Barragan L, Kuri T, Blakqori G, Weber F, Ludewig B, Thiel V.** 2007.
526 Coronavirus non-structural protein 1 is a major pathogenicity factor: implications for the rational
527 design of coronavirus vaccines. *PLoS pathogens* **3**:e109.
- 528 35. **Vervelde L, Matthijs MG, van Haarlem DA, de Wit JJ, Jansen CA.** 2013. Rapid NK-cell activation
529 in chicken after infection with infectious bronchitis virus M41. *Vet Immunol Immunopathol* **151**:337-
530 341.
- 531 36. **Zhou H, Perlman S.** 2006. Preferential infection of mature dendritic cells by mouse hepatitis virus
532 strain JHM. *J Virol* **80**:2506-2514.
- 533 37. **Cinatl J, Morgenstern B, Bauer G, Chandra P, Rabenau H, Doerr HW.** 2003. Treatment of SARS
534 with human interferons. *Lancet* **362**:293-294.
- 535 38. **Zheng B, He ML, Wong KL, Lum CT, Poon LL, Peng Y, Guan Y, Lin MC, Kung HF.** 2004. Potent
536 inhibition of SARS-associated coronavirus (SCOV) infection and replication by type I interferons (IFN-
537 alpha/beta) but not by type II interferon (IFN-gamma). *J Interferon Cytokine Res* **24**:388-390.
- 538 39. **Yoshikawa T, Hill TE, Yoshikawa N, Popov VL, Galindo CL, Garner HR, Peters CJ, Tseng CT.**
539 2010. Dynamic innate immune responses of human bronchial epithelial cells to severe acute
540 respiratory syndrome-associated coronavirus infection. *PLoS One* **5**:e8729.
- 541 40. **Wathelet MG, Orr M, Frieman MB, Baric RS.** 2007. Severe acute respiratory syndrome coronavirus
542 evades antiviral signaling: role of nsp1 and rational design of an attenuated strain. *J Virol* **81**:11620-
543 11633.
- 544 41. **Cruz JL, Becares M, Sola I, Oliveros JC, Enjuanes L, Zuniga S.** 2013. Alphacoronavirus protein 7
545 modulates host innate immune response. *J Virol* **87**:9754-9767.
- 546 42. **Kindler E, Thiel V.** 2014. To sense or not to sense viral RNA: essentials of coronavirus innate immune
547 evasion. *Current Opinion in Microbiology* **20**:69-75.
- 548 43. **Zhang R, Jha BK, Ogden KM, Dong B, Zhao L, Elliott R, Patton JT, Silverman RH, Weiss SR.**
549 2013. Homologous 2',5'-phosphodiesterases from disparate RNA viruses antagonize antiviral innate
550 immunity. *Proc Natl Acad Sci U S A* doi: 10.1073/pnas.1306917110.
- 551 44. **Davies MT.** 2009. Subcellular location and protein interactions of the infectious bronchitis virus gene 3
552 and 5 accessory proteins University of Warwick.
- 553 45. **Knoops K, Kikkert M, Worm SH, Zevenhoven-Dobbe JC, van der Meer Y, Koster AJ, Mommaas**
554 **AM, Snijder EJ.** 2008. SARS-coronavirus replication is supported by a reticulovesicular network of
555 modified endoplasmic reticulum. *PLoS Biol* **6**:e226.
- 556 46. **Ulasli M, Verheije MH, de Haan CA, Reggiori F.** 2010. Qualitative and quantitative ultrastructural
557 analysis of the membrane rearrangements induced by coronavirus. *Cell Microbiol* **12**:844-861.
- 558 47. **Maier HJ, Hawes PC, Cottam EM, Mantell J, Verkade P, Monaghan P, Wileman T, Britton P.**
559 2013. Infectious Bronchitis Virus Generates Spherules from Zippered Endoplasmic Reticulum
560 Membranes. *mBio* **4**.
- 561 48. **Lundin A, Dijkman R, Bergström T, Kann N, Adamiak B, Hannoun C, Kindler E, Jónsdóttir HR,**
562 **Muth D, Kint J, Forlenza M, Müller MA, Drosten C, Thiel V, Trybala E.** 2014. Targeting
563 Membrane-Bound Viral RNA Synthesis Reveals Potent Inhibition of Diverse Coronaviruses Including the
564 Middle East Respiratory Syndrome Virus. *PLoS Pathog* **10**:e1004166.
- 565 49. **van Hemert MJ, van den Worm SH, Knoops K, Mommaas AM, Gorbalenya AE, Snijder EJ.**
566 2008. SARS-coronavirus replication/transcription complexes are membrane-protected and need a host
567 factor for activity in vitro. *PLoS Pathog* **4**:e1000054.
- 568 50. **Neuman BW, Angelini MM, Buchmeier MJ.** 2014. Does form meet function in the coronavirus
569 replicative organelle? *Trends Microbiol* doi: 10.1016/j.tim.2014.06.003.
- 570 51. **Versteeg GA, Bredenbeek PJ, van den Worm SH, Spaan WJ.** 2007. Group 2 coronaviruses
571 prevent immediate early interferon induction by protection of viral RNA from host cell recognition.
572 *Virology* **361**:18-26.
- 573 52. **Zhou H, Perlman S.** 2007. Mouse hepatitis virus does not induce Beta interferon synthesis and does
574 not inhibit its induction by double-stranded RNA. *Journal of virology* **81**:568-574.

575

576 **Figure legends**577 **FIG 1 Accessory protein 3a confers resistance to treatment of IBV with type I IFN**

578 (A) Primary chicken embryo kidney (CEK) cells and Vero cells were pre-stimulated with IFN (1000
579 U/ml) for 6 h and subsequently infected with Sindbis virus (SinV) or IBV (Beau-R) at MOI 0.1. At
580 24 hpi, cells were fixed and stained for dsRNA (red) or IBV-N (green). (B) CEK cells were pre-
581 stimulated with the indicated concentration of IFN for 6 h, and subsequently infected with Beau-R
582 (MOI 0.01). At 2 hpi, cells were washed to remove inoculum, and medium with IFN was added. At
583 18hpi supernatant was sampled and titrated (see also inset for sampling time line). Symbols
584 represent the mean of triplicate measurements (\pm SEM) of virus titers from two independent
585 experiments. The asterisk (*) indicates significant differences ($P < 0.05$) between IFN α and IFN β
586 treatment as assessed by a two-way ANOVA. (C) CEK cells were IFN-treated, virus-infected and
587 sampled at 18hpi as described under (B), using Beau-R and accessory protein-null viruses (MOI
588 0.01). Titers were determined at 18 hpi and are expressed relative to titers of non-IFN-treated
589 wells. The lower the value, the higher the reduction. Symbols indicate the mean (\pm SEM) of
590 triplicate measurements from two independent experiments. Asterisk (***) indicates significant
591 difference ($P < 0.001$) compared to Beau-R as assessed by one-way ANOVA followed by a
592 Bonferroni post-hoc test. Titers in non-IFN treated wells are displayed for each virus. (D) CEK cells
593 were infected with the indicated viruses (MOI 10) and at 2 hpi, inoculum was removed and cells
594 were incubated with IFN (10,000 U/ml). Virus titers in the supernatant were determined at 18 hpi,
595 and are expressed as fold change relative non-IFN-treated wells infected with the same virus (see
596 also inset for sampling time line). (E and F) DF-1 cells were IFN-treated and virus-infected as
597 described in (B). Symbols indicate the mean relative titer at 24 hpi (\pm SEM) of triplicate wells from
598 a representative experiment of two biological replicates. Asterisks (**) indicate significant
599 differences ($P < 0.01$) between ScAUG3ab virus and the other viruses as assessed by a two-way
600 ANOVA. (G) DF-1 cells were IFN-treated and virus-infected as described under (B). Bars represent
601 the fold change in virus titer at 24 hpi (\pm SD) of triplicate wells from two biological replicates.
602 Asterisks indicate significant differences (*, $P < 0.05$; **, $P < 0.01$; ***, $P < 0.001$) to Beau-R, as
603 assessed by a one-way ANOVA followed by a Bonferroni post-hoc test. (H and I) DF-1 cells were
604 IFN-treated and virus-infected as described under (B). At 24 hpi, total RNA was extracted from the
605 cell culture supernatant and virus RNA was quantified by RT-qPCR using primers against the N-
606 gene. Values are expressed as a fold change relative non-IFN-treated wells, infected with the same
607 virus. The lower the value, the higher the reduction of viral RNA. Symbols represent the mean of

608 quadruplicate wells (\pm SD) from one experiment. Letters indicate significant differences at the
609 highest IFN concentration as assessed by a one-way ANOVA followed by a Tukey post-hoc test.
610

611 **FIG 2 IBV prevents translocation of STAT1 and IFN signalling at late stages of infection.**
612 (A) Vero cells were infected with IBV-Beau-R (MOI 1 for 6h and MOI 0.1 for all other time points)
613 and subsequently stimulated with 1000 U/ml IFN β for 30 min before fixation and staining for IBV-N
614 and STAT1. White arrowheads indicate nuclear accumulation of STAT1, black arrowheads indicate
615 absence of STAT1 accumulation in the nucleus. (B) Cells were treated as in A, and at the indicated
616 time points after IBV infection, the percentage of nuclei showing translocation of STAT1 (black
617 bars) or not (white bars) was determined in non-infected (non-inf.) and in IBV-infected (IBV-inf)
618 cells within IFN β -treated wells. Each bar indicates the mean percentage of nuclei showing
619 translocation of STAT1 as determined in 50 - 400 cells from multiple images of a representative
620 experiment of two biological replicates. Error bars indicate standard deviation (SD). (C) DF-1 cells
621 were transfected with an ISG54-Firefly luciferase construct, and 24 hours later infected with Beau-
622 R or SinV (MOI 5 and 0.5, respectively); at 6 or 18 hpi, cells were stimulated with 1000 U/ml IFN β
623 for an additional 6h. ISG54 promotor activity was calculated as percentage relative to non-IFN β -
624 treated wells. Shown is the ISG54 promotor activity in non-infected-IFN β -treated wells (striped
625 bar) and in IBV-infected-IFN β -treated wells at 12 and 24 hpi (black bars). Firefly luciferase values
626 were normalised to SV40-Renilla luciferase to correct for differences in transfection efficiency and
627 protein translation. Bars indicate the mean (+ SD) of triplicate wells from a representative
628 experiment out of three biological replicates. Asterisks (***) indicate significant differences ($P <$
629 0.001) with respect to non-infected cells, as assessed by one-way ANOVA followed by a Bonferroni
630 post-hoc test.
631

632 **FIG 3 IBV prevents translocation and phosphorylation of STAT1**

633 Vero cells were infected for 18 h with IBV Beau-R (MOI 0.1) and subsequently stimulated with
634 1000 U/ml IFN β for 30 min. (A) westernblot analysis of non-infected (non-inf.) and IBV-infected
635 monolayers that were either mock- or IFN β -treated. Staining was performed using antibodies
636 against STAT1 and Tyr701-phosphorylated STAT1. Staining against β -Tubulin was included as a
637 loading control. Numbers below the blots indicate the intensity of the band, expressed as fold ratio
638 relative to the IFN β -stimulated, non-infected sample. (B) Vero cells treated as described above
639 were fixed and stained for IBV-N and pSTAT1. White arrowheads indicate translocation of pSTAT1,
640 black arrowheads indicate absence of pSTAT1 from the nucleus. (C) To verify the overall decrease
641 of pSTAT1, an area containing IBV-infected cells within an IFN β -stimulated monolayer is delineated
642 by a dotted line in the top left panel and is overlaid on the bottom left panel to illustrate the
643 absence of pSTAT1 in IBV-infected cells. Cross section: fluorescence intensity plot of pSTAT1 and
644 IBV-N along the yellow line indicated in the top right panel.

645

646 **FIG 4 IBV accessory proteins are not required for inhibition of STAT1 translocation and**
647 **ISG promotor activation.**

648 (A) Western blot analysis of IBV-infected (MOI 1, 18 hpi) and non-infected Vero cells that were
649 either mock- or IFN β -treated for 30 min. Staining was performed using an antibody against
650 Tyr701-phosphorylated STAT1, and an antibody against β -tubulin was used as loading control. (B)
651 Vero cells were infected with the indicated viruses (MOI 0.1) and at 18 hpi, stimulated with 1000
652 U/ml IFN β for 30 min, and stained for IBV-N and pSTAT1. The area delineated by the yellow dotted
653 line indicates the overall decrease in pSTAT1 staining in IBV-infected cells. (C) Vero cells were
654 infected with Beau-R, ScaUG3ab or ScaUG5ab viruses (MOI of 0.1) and at 18 hpi, stimulated with
655 1000 U/ml IFN β for 30 min, and stained for IBV-N and pSTAT1. White arrowheads indicate
656 translocation of pSTAT1, black arrowheads indicate absence of accumulation of pSTAT1 in the
657 nucleus. (D) In parallel, the percentage of nuclei showing translocation of STAT1 (black bars) or
658 not (white bars) was determined in non-infected (non-inf.) and in IBV-infected (IBV-inf.) cells
659 within IFN β -treated wells. Each bar indicates the mean (+ SD) percentage of nuclei showing
660 translocation based on 100 - 300 cells from multiple images of a representative experiment of two
661 biological replicates. Asterisks (**) indicate significant differences ($P < 0.01$) with respect to non-
662 infected cells, as assessed by one-way ANOVA followed by a Bonferroni post-hoc test. (E)
663 Quantification of the percentage of IBV-infected cells in microscopic images of cells infected with
664 the indicated viruses at MOI 0.1 and stained using IBV-N-specific antibody at 18 hpi. For each
665 virus, at least 500 cells divided over 10 microscopic fields were analysed. (F) Virus titres in
666 supernatants from Vero cells infected for 18 h with the indicated viruses at MOI 0.01. (G) Vero and
667 DF-1 cells were transfected with an ISG54-Firefly luciferase construct, and 24 h later infected with
668 Beau-R, ScaUG3ab or ScaUG5ab viruses at MOIs 5, 0.5, 0.05. At 18 hpi, cells were stimulated with
669 1000 U/ml IFN β for an additional 6 h. After a total of 24 h, Firefly and Renilla luciferase activity was
670 quantified. ISG54 promotor-activity was calculated as percentage relative to non-IFN β -treated
671 wells. Shown is the ISG54 promotor-activity in non-infected, IFN β -treated wells (striped bar) and
672 in IBV-infected, IFN β -treated wells (black bars). Firefly luciferase values were normalised to SV40-
673 Renilla luciferase to correct for differences in transfection efficiency and protein translation. Bars
674 indicate the mean (+ SD) of triplicate wells of a representative example of n=3 biological
675 replicates.

FIG 1

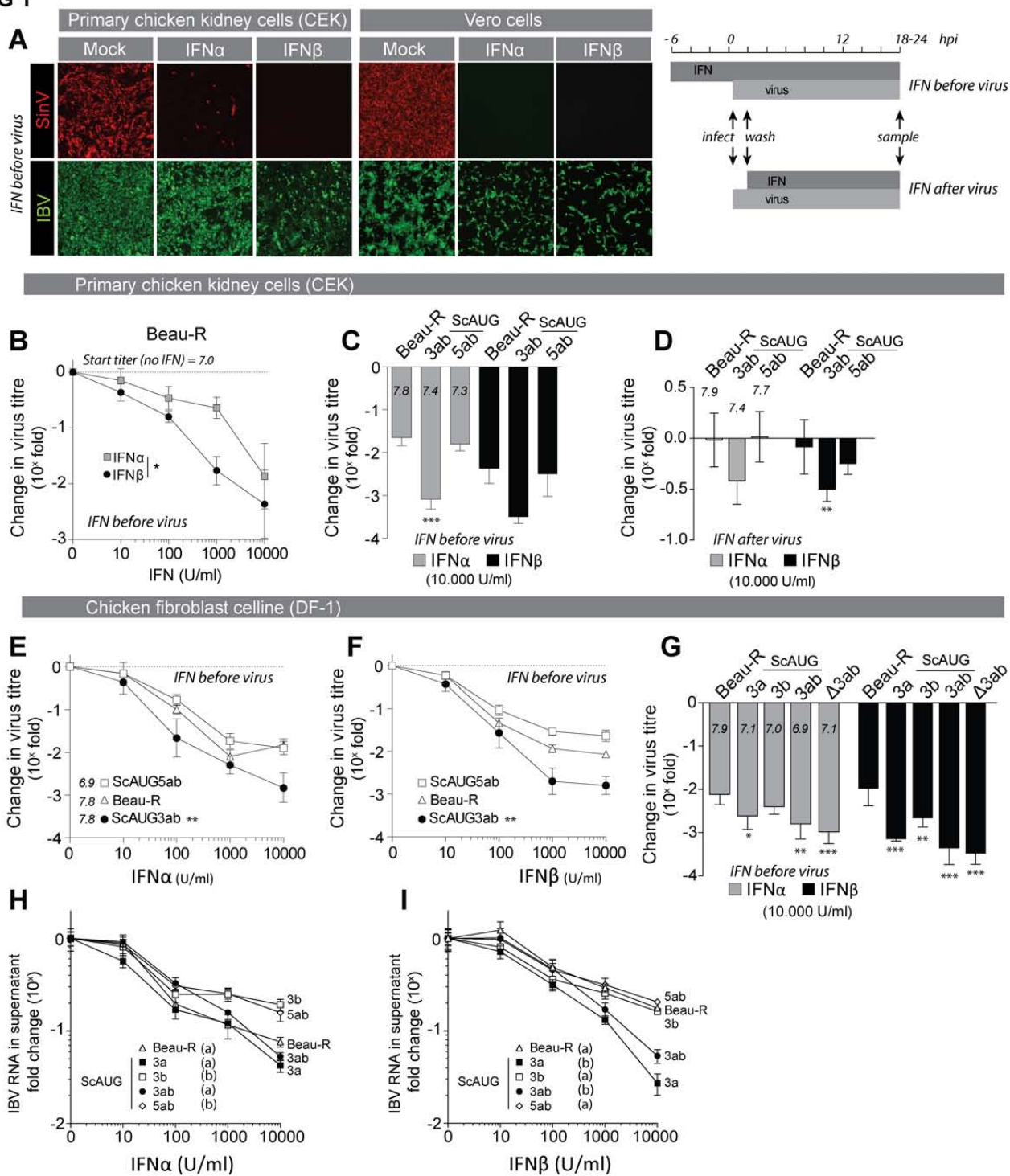


FIG 2

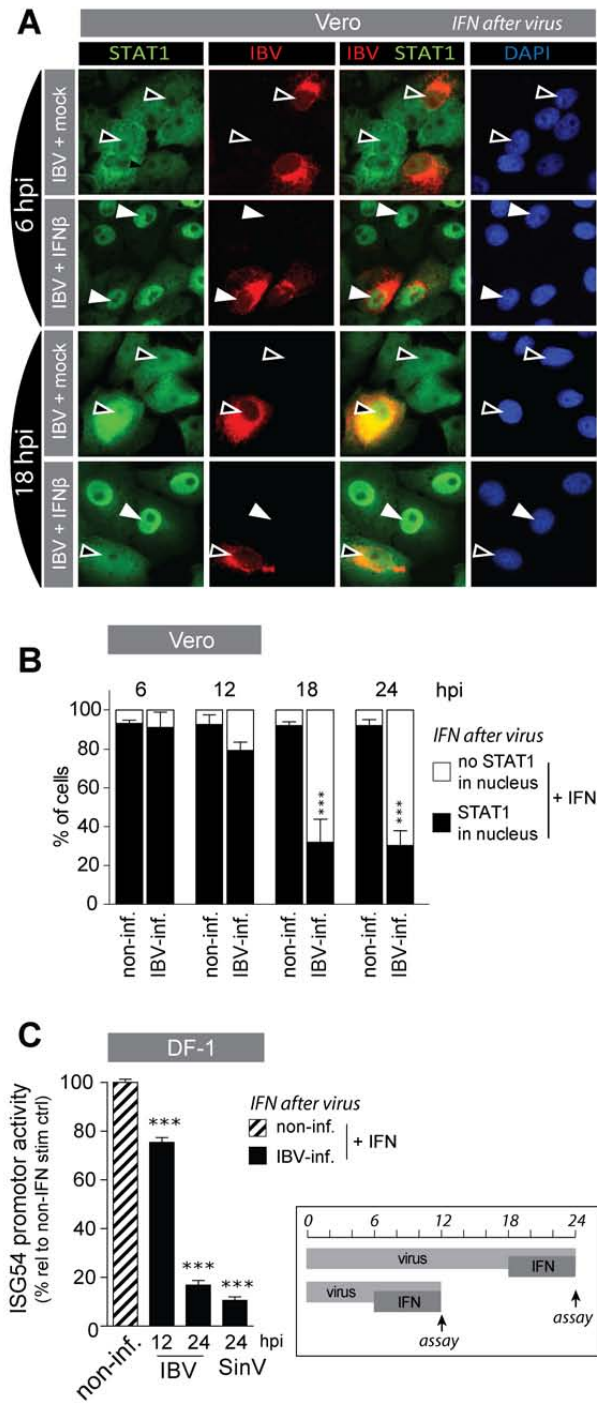


FIG 3

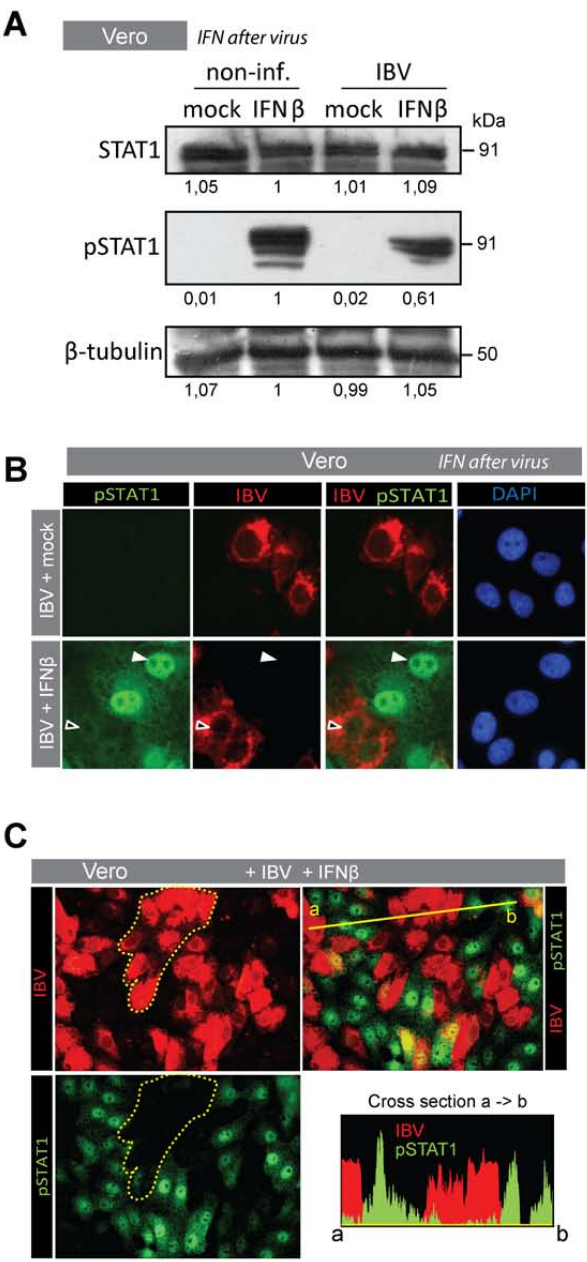


Fig 4

